Inhibition of GTP-dependent vesicle trafficking impairs internalization of plasmalemmal eNOS and cellular nitric oxide production

Suvro Chatterjee[1], Sheng Cao[1], Timothy E. Peterson[2], Robert D. Simari[2] and Vijay Shah[1,*]

[1]GI Research Unit, Department of Physiology, and Tumor Biology Program, Mayo Clinic, Rochester, MN 55905, USA
[2]Division of Cardiovascular Disease, and Molecular Medicine Program, Mayo Clinic, Rochester, MN 55905, USA
*Author for correspondence (e-mail: shah.vijay@mayo.edu)

Accepted 12 May 2003
Journal of Cell Science 116, 3645-3655 © 2003 The Company of Biologists Ltd
doi:10.1242/jcs.00664

Summary

The Ca^{2+} mobilizing peptide, bradykinin (BK), stimulates endothelial nitric oxide synthase (eNOS)-derived cellular nitric oxide (NO) production in association with altering the subcellular distribution of the enzyme. In the present study we examine the influence of cellular GTPases, particularly the large GTPase dynamin, on BK-mediated eNOS localization and cellular NO production. BK stimulation of ECV cells, which were stably transfected with eNOS-GFP (eNOS-GFP ECV304), increased NO production. This was associated with the mobilization of eNOS-GFP protein into Triton X-100-insoluble fractions of cell lysates, and an internalization of plasmalemmal eNOS-GFP in live and fixed ECV 304 cells. Incubation of digitonin-permeabilized ECV304 cells with the non-hydrolyzed GTP analog, GTP-γ-S, abrogated the BK-mediated internalization of eNOS-GFP as assessed by confocal microscopy. Conversely, inhibition of clathrin-dependent endocytosis, via overexpression of AP 180 or pretreatment of cells with chlorpromazine, did not influence BK-mediated eNOS redistribution. Furthermore, specific inhibition of dynamin-2 GTPase function by overexpression of a dominant negative construct, K44A, prevented the BK-mediated enrichment of eNOS-GFP within low buoyant density, caveolin-enriched fractions of eNOS-GFP ECV304 cell lysates. Dynamin-2 K44A overexpression also markedly impaired BK-dependent, L-NAME-inhibited NO production as did incubation of permeabilized cells with GTP-γ-s. These studies demonstrate that disruption of dynamin- and GTP-dependent, but clathrin-independent, vesicle trafficking pathways impairs BK-dependent cellular NO production, via inhibition of the internalization of eNOS-containing plasmalemmal vesicles.

Key words: Nitric oxide, Nitric oxide synthase, Bradykinin, Dynamin-2

Introduction

Endothelial nitric oxide synthase (eNOS) and its enzymatic byproduct, nitric oxide (NO), are integral to numerous vascular functions including vasodilation and vascular remodeling (Palmer et al., 1987; Rudic, 1998; Shaul, 2002). In this regard, eNOS derived NO production is regulated at multiple cellular levels including transcription, post-transcription and post-translation (Papapetropoulos et al., 1999). With regard to the last of these mechanisms, the appropriate subcellular targeting of eNOS within the membrane compartment of cells is necessary for optimizing cellular NO production (Blair et al., 1999; Fulton et al., 2002; Shaul et al., 1996). Membrane targeting, predominantly to plasmalemmal caveolae and Golgi membranes, has been ascribed to a number of processes including amino-terminal acylation, sequence-specific binding of eNOS protein with specific membrane-spanning proteins such as caveolin and chaperone molecules (Blair et al., 1999; Fulton et al., 2002; Liu et al., 1995; Prabhakar et al., 2000; Shaul et al., 1996). As an extension to this concept, previous studies have demonstrated that cellular eNOS localization is influenced by both cellular homeostatic conditions such as cell confluency state and receptor-mediated inhibitory and excitatory signaling stimuli such as oxidized low density lipoproteins and bradykinin (BK) (Michel et al., 1993; Blair et al., 1999; Prabhakar et al., 1998; Sowa et al., 1999; Thuringer et al., 2002).

BK is a soluble peptide that acts via NO to promote vasodilation and capillary permeability. Soluble BK binds the membrane-bound BK2 receptor with downstream activation of eNOS through divergent and convergent signaling pathways that include Hsp 90, MAP kinase, receptor tyrosine kinases, and eNOS dephosphorylation (Bernier et al., 2000; Harris et al., 2001; Thuringer et al., 2002; Venema et al., 1996). In addition to these complimentary signaling pathways, it has been observed that treatment of cells with BK is associated with changes in the subcellular distribution of eNOS (Prabhakar et al., 1998; Thuringer et al., 2002; Venema et al., 1996). Owing to the prominent influence of GTPases, particularly the large GTPase, dynamin-2, on internalization of plasmalemmal vesicles and downstream signaling pathways such as that described for the extracellular signal-regulated kinase cascade (Pierce et al., 1999), we sought to determine the influence of perturbation of dynamin-2 and GTP hydrolysis on cellular eNOS localization and NO production. We hypothesized that the specific targeting of eNOS, as a passive cargo within cellular vesicles, may influence the ability of the

enzyme to produce and release NO. We demonstrate, using two complimentary cell systems, that BK-stimulated NO production is associated with a redistribution of the plasmalemmal pool of eNOS protein, with enrichment within Triton X-100 insoluble, low buoyant density cell fractions. Furthermore, we demonstrate that disruption of dynamin- and GTP-dependent endocytosis, but not clathrin-dependent endocytosis, abrogates the BK-mediated redistribution of eNOS within cells. Also, disruption of dynamin GTP hydrolysis attenuates BK-dependent cellular NO production. These studies implicate a role for GTPase-dependent, clathrin-independent, trafficking of eNOS-containing vesicles in the mechanism of BK-mediated NO generation.

Materials and Methods

Materials and antibodies

All tissue culture and transfection reagents were obtained from GIBCO BRL. eNOS mAb, caveolin pAb, were obtained from Transduction Laboratories (Lexington, KY, USA), β-COP pAb was from Affinity Bioreagents, Inc (Golden, CO, USA), Golgi 58K mAb and plasma membrane marker, Na^+-K^+ ATPase mAb were from Sigma (St Louis, MO), and myc and V5 mAb were from Invitrogen Life Technologies (Carlsbad, CA, USA). Texas Red-conjugated transferrin was from Rockland Immunochemicals (Gilbertsville, PA). A polyclonal antibody that specifically recognizes dynamin-2 (dyn2T) was a generous gift from Dr Mark McNiven (Henley et al., 1998). Optiprep, was obtained from Nycomed Pharma AS (Oslo, Norway). The K44A dominant negative dynamin-2 cDNA, which contains a point mutation in the GTP binding element, thereby preventing GTP hydrolysis, a kind gift from Dr Mark McNiven, was subcloned into pcDNA3 in frame with a V5 epitope tag. The myc-tagged AP 180 cDNA in pCMV was a generous gift from Dr H. McMahon (Ford et al., 2001). The probes, DAF-2 and DAF-2DA, for the fluorimetric detection of NO, were obtained from Calbiochem (La Jolla, CA)

Cell culture

Complimentary techniques were performed in both bovine aortic endothelial cells (BAEC), which express eNOS endogenously, and in ECV-304 cells stably transfected with eNOS-GFP (eNOS-GFP ECV 304 cells) (Sowa et al., 1999). Although the latter cells are probably derived from a human bladder tumor (Brown et al., 2000), their phenotype has been documented to partially overlap with that of endothelial cells; and owing to their stable and uniform expression of eNOS-GFP at relatively high levels (Paxinou et al., 2001; Sowa et al., 1999), these cells have served as a useful model in which to study eNOS trafficking. BAEC were from Clonetics (San Diego, CA) and used between P2 and P5, while eNOS-GFP-ECV 304 cells were a generous gift from Dr William Sessa (Sowa et al., 1999). Both cell types were cultured in Dulbecco's modified Eagle's medium (DMEM), supplemented with 10% fetal bovine serum; 1 mM L-glutamine, and 100 IU/ml penicillin. eNOS-GFP ECV 304 cells were additionally supplemented with 400 μg/ml G418. For transfection experiments, eNOS-GFP ECV 304 cells were plated on glass coverslips in 12- or 24-well plates, or in 100 mm culture dishes and transfected using a calcium phosphate method with pcDNA3-dyn 2 K44A, pCMV-myc AP 180, or appropriate control vectors. Twenty-four hours after transfection of eNOS-GFP ECV 304 or 24 hours after plating of BAEC, the cells were incubated with 10 μM BK or vehicle for 10 minutes at 37°C. After BK stimulation, cells were prepared for various subcellular fractionation procedures, microscopic analyses, or NO measurements as individually described below. For permeabilization experiments, cells were pretreated with either 1 μM digitonin, 10 μM GTP-γ-s, 1 μM digitonin plus 10 μM GTP-γ-s, or vehicle (PBS) for 5 minutes, then washed with PBS prior to BK stimulation. In some experiments 10 μM ATP-γ-s was used in place of GTP-γ-s and in some experiments, cells were treated with 15 μM chlorpromazine (CP), an agent that blocks clathrin-dependent endocytosis, for 10 minutes prior to BK stimulation (Petris et al., 2002). To assess transferrin uptake in response to AP 180 transfection (Ford et al., 2001), cells were incubated in low serum medium (0.2% BSA) for 30 minutes at 37°C and Texas Red-conjugated transferrin was added from a stock of 5 mg/ml to the medium at a ratio of 1:1000. Cells were washed with PBS after 10 minutes incubation at 37°C. Cells were washed further with low serum medium (pH 3.5) to reduce background signals and fixed with 2% formaldehyde solution. Uptake of transferrin was assessed by confocal laser scanning microscopy.

Confocal laser scanning microscopy

To study eNOS-GFP localization in living cells in response to BK stimulation, a cell culture system with stable temperature control (POC-R; Zeiss) was mounted to the laser scanning confocal microscope (Pasqual LSM 5; Zeiss). Briefly, eNOS-GFP ECV 304 cells plated and cultured on 32 mm coverslips were mounted in fresh medium in the 37°C POC-R chamber on the microscope. BK was added to the chamber and the cells were scanned and single confocal images were captured at 4-minute intervals using a 63× C-apochromat lens. Micrographs of live cells were digitized and exported to Adobe Photoshop, version 5.0, for calculation of the intensity of the fluorescence in the perinuclear and plasmalemmal regions at each time interval, using data pooled from three independent experiments. For immunofluorescence microscopic analysis, BAEC were fixed in acetone/methanol 1:1 for 3 minutes at –20°C after BK stimulation (10 minutes), while ECV 304 cells were fixed with 2% paraformaldehyde. Fixed cells were incubated with the appropriate dilution of indicated Ab or blocking serum for 2 hours at room temperature, and primary Ab was detected with an FITC- or Texas Red-conjugated secondary antibody and mounted in Anti-fade (Molecular Probes, Oregon). Cells were visualized using a confocal laser scanning microscope with a 63× lens. Owing to the previously noted heterogeneity in subcellular distribution of eNOS between neighboring cells (Prabhakar et al., 1998; Sowa et al., 1999), we classified cells into two groups for the purpose of quantifying changes in NOS distribution in association with BK: (1) plasma membrane pattern (*PM*: cells with distinct plasma membrane and perinuclear localization of eNOS-GFP) and (2) non-plasma membrane pattern (*Non PM*: cells with perinuclear localization of eNOS-GFP in the absence of plasmalemmal staining). Quantification of eNOS redistribution in fixed cells was performed in a blind fashion from 200 individual cells in each group from two independent experimental preparations.

Measurement of cellular NO production

NO production was measured using the complimentary fluorescent NO indicator probes, DAF 2DA and DAF-2, the former detects intracellular NO accumulation and the latter detects NO production by assessing NO released from cells (Fulton et al., 2002; Goetz et al., 1999; Kojima et al., 1998), as well as NO-specific chemiluminescence (Shah et al., 1997). For the DAF-2DA assay, BAEC were cultured on glass coverslips in 12-well plates. After the permeabilization procedure described above, cells from each of the experimental groups were washed twice with PBS, preincubated with 0.1 mM NOS substrate, L-arginine at 37°C, or 1.0 mM of the NOS inhibitor, L-NAME for 10 minutes, then loaded with DAF-2DA (10 μM). After 10 minutes, BK or vehicle was added to the cells. Intracellular DAF-2DA fluorescence was visualized using a conventional fluorescence microscope (5100TV, Zeiss, Germany) and fluorescence was quantified from ten selected regions of the digitized micrographs, each taken at 1 minute time intervals, using Adobe Photoshop 5.0 software. Specificity of DAF-2DA fluorescence was established in preliminary

experiments, which demonstrated a linear relationship between DAF-2DA fluorescence intensity in response to the NO-stimulating calcium ionophore A23187 and parallel control experiments using DAF-4, a nonfluorescent analog (data not shown). To measure cellular NO release using DAF-2, eNOS-GFP ECV304 cells were transfected as described above and 24 hours later cells were incubated in a solution containing 1 μM DAF-2 with either 0.1 mM L-arginine or 1 mM L-NAME at 37°C. After 30 minutes, BK (10 μM) was added to the cells for an additional 10 minutes at which point the cell supernatant was transferred to microcuvettes for fluorescence quantification with excitation of 485 nm and emission of 538 nm using a fluorimeter (VersaFluor Flurometer, BioRad). Fluorimetry was performed with duplicate readings from duplicate wells and run along side a standard curve generated using known amounts of sodium nitroprusside (0-500 nM) and normalized for cellular protein.

NO-specific chemiluminescence was performed using a Seivers NOA, essentially as previously described (Shah et al., 1997), except that glacial acetic acid containing sodium iodine was substituted for vanadium/hydrochloric acid as the refluxing agent. A standard curve was generated using known nitrite standards. Samples of medium were measured in duplicate and normalized for protein concentration.

Subcellular fractionation and western blotting

For separation of cell membranes from cytosol, BAEC or eNOS-GFP ECV 304 cells were scraped in a buffer containing 50 mM Tris-HCl pH 7.4, 0.1 mM EDTA, 0.1 mM EGTA, plus a protease inhibitor cocktail (Roche Diagnostics, Germany), and sonicated on ice at 200 W/cm^2 for 3 cycles with 10 seconds intervals, then centrifuged at 100,000 ***g*** for 1 hour at 4°C. The pellet constituted the membrane fraction and the supernatant was utilized as the cytosolic fraction. Equal amounts of protein from the membrane and cytosol fractions were boiled in Laemmli buffer for 5 minutes and subjected to SDS-PAGE and western blotting. In experiments examining eNOS segregation in response to Triton X-100, the membrane pellet was resuspended in 0.5% Triton X-100 in 50 mM Tris-HCl buffer for 15 minutes at 4°C and centrifuged at 10,000 ***g*** for 10 minutes. The resulting pellet constituted the Triton insoluble fraction (TIF) while the supernatant represented the Triton soluble fraction (TS). The TIF membrane pellet was homogenized with 5 cycles of 20 strokes in a Dounce homogenizer. Protein concentrations of these fractions were determined by BCA assay and equal aliquots were boiled in Laemmli buffer and subjected to SDS-PAGE and western blotting. Cellular proteins were also fractionated by buoyant density, using a well established protocol (Smart et al., 1995) that we have slightly modified as we previously described (Peterson et al., 1999). For separation of low buoyant density membranes, four 150 mm dishes of confluent eNOS-GFP ECV 304 cells were washed and scraped in 5 ml of fractionation buffer (0.25 M sucrose, 6 mM EDTA, 120 mM Tricine, pH 7.8) and pelleted by centrifugation (1400 ***g***). Cells were resuspended in 1 ml of the identical buffer and homogenized with 20 strokes of a Dounce homogenizer. A postnuclear supernatant was collected by centrifugation for 10 minutes at 1000 ***g***. The supernatant was layered on 30% Percoll in fractionation buffer and centrifuged at 84,000 ***g*** for 30 minutes. A distinct visible band comprising plasma membranes was collected and sonicated three times (200 W/cm^2). Sonicated samples were mixed with Optiprep to a final concentration of 23%, in a Sorvall Ultrafuge tube. Two additional layers of 20% and 10% Optiprep were added prior to centrifugation at 52,000 ***g*** for 90 minutes. Eight gradient fractions were collected and 30 μl of each fraction were boiled in Laemmli buffer for 5 minutes and used for SDS-PAGE. After cell fractionation and SDS-PAGE, gels were prepared for Coommassie staining or alternatively for transfer to nitrocellulose membranes for western blotting. For western blotting, membranes were blocked with 5% dry milk for 1 hour at room temperature prior to incubation with antibodies specific for eNOS, caveolin, β-COP, dynamin-2, myc and V5 epitope as previously described (Shah et al., 1999).

Statistical analysis

Where appropriate, analysis of variance (two-tailed, paired values) was used to evaluate the differences in the levels of parameters studied, using Statgraff, Version 3. A P value of 0.05 was considered statistically significant.

Results

Bradykinin-induced cellular NO production is associated with a temporal redistribution of eNOS

BK acts through the membrane-bound BK2 receptor to stimulate NO production through well delineated signaling pathways, which are associated with a redistribution of eNOS protein (Bernier et al., 2000; Harris et al., 2001; Prabhakar et al., 1998; Thuringer et al., 2002; Venema et al., 1996). To examine this model, we stimulated eNOS-GFP ECV 304 cells with BK (10 μM) and examined NO production and subcellular localization of eNOS. First, we measured BK-induced production of NO in live cells using the complimentary fluorescence compounds DAF-2 and DAF-2DA, which assess NO production by estimating extracellular NO release and intracellular accumulation of NO, respectively. eNOS-GFP ECV 304 cells generated NO in a BK-dependent manner, and L-NAME-inhibitable manner, as assessed by DAF-2 fluorimetry (Fig. 1, left panel). Corroborative results were obtained in BAEC loaded with DAF-2DA, as assessed by quantification of fluorescence intensity from digitized images of cells stimulated with BK (10 μM) in the presence of L-arginine or alternatively, L-NAME (Fig. 1, right). These studies establish the NO stimulatory effect of BK and demonstrate the specificity of the DAF fluorescent compounds in these experimental conditions and cell systems.

To examine the influence of BK on eNOS subcellular distribution, we performed biochemical and microscopic analyses. First, eNOS-GFP ECV 304 cells were stimulated with BK (10 μM) or vehicle for 10 minutes, and cell lysates were separated into cytosolic and membrane fractions. Western blot analysis of these fractions did not demonstrate differences in distribution of eNOS between these two fractions in cells treated with BK as compared to vehicle, as previously reported (Liu et al., 1995). However, further separation of the membrane pellet by Triton X-100 solubility revealed an enrichment of eNOS protein within the Triton-insoluble fraction of cells treated with BK as compared to vehicle (Fig. 2, right).

We next assessed the influence of BK on eNOS localization by performing studies in live eNOS-GFP ECV 304 cells using a cell culture system adapted for a laser scanning confocal microscope. Previous studies in these cells have established that tracking of GFP accurately assesses, and does not confound, the subcellular localization of the fused eNOS protein (Sowa et al., 1999). Treatment of eNOS-GFP ECV 304 cells with BK promoted the time-dependent internalization of eNOS from the plasmalemmal eNOS location that is characteristic of these cells when grown to confluence (Fig. 3A, bottom panel micrographs). Temporal quantification of fluorescence intensity of both Golgi and plasmalemmal pools of eNOS demonstrate that Golgi distribution of eNOS did not decrease in parallel with the plasmalemmal pool of eNOS,

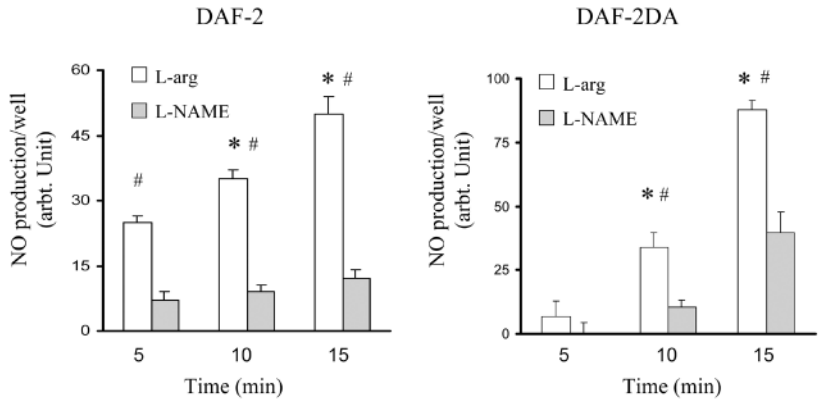

Fig. 1. BK stimulates cellular NO production. BK-mediated cellular NO production was measured from eNOS-GFP ECV 304 cells and BAEC using the cell membrane-impermeable and -permeable fluorescent probes, DAF-2 and DAF-2DA, respectively. Cells were cultured in 12-well plates for 24 hours and then culture medium was replaced with PBS containing L-arginine (0.1 mM) or alternatively, L-NAME (1 mM) for 30 minutes, loaded with either DAF-2 or DAF-2DA, then stimulated with BK (10 μM). Relative NO production was measured by fluorimetry from the media for DAF-2 experiments and alternatively assessed by quantitation of fluorescence intensity from captured microscopic images for DAF-2DA experiments. eNOS-GFP ECV 304 cells preincubated with L-arginine produced NO in a time-dependent manner after BK stimulation, as assessed by increased DAF-2 fluorescence in the medium (left panel), as do BAEC, as assessed by increased intracellular DAF-2DA fluorescence (right panel) (n=10 selected areas from each micrograph from 3 independent experiments; *P<0.05 compared to 5 minutes). In both cell types, BK stimulation of NO production was markedly inhibited by L-NAME preincubation (1 mM) (n=3 independent DAF-2 experiments each performed in duplicate; $^{\#}P$<0.05 compared to L-NAME).

reducing the likelihood of a photobleaching effect (Fig. 3A, graph in bottom panel). Cells treated with vehicle showed no change in the fluorescence pattern of eNOS-GFP over a similar time period indicating that eNOS localization was not influenced by the cell culture conditions within the experimental system (Fig. 3A, top panel, micrographs and graph). The graphs were generated by compiling cumulative data points from 3 cells from each group (mean ± s.e.m.).

Next, to further demonstrate that eNOS does indeed leave the plasma membrane in response to BK, immuno-localization studies of plasma membrane and Golgi marker proteins were performed in conjunction with eNOS localization in fixed cells after BK stimulation. As seen in Fig. 3B (top panels), Na^+-K^+ ATPase immunolocalization is detected on the plasma membrane of cells (top left panel), and substantive pools of eNOS are situated on the plasma membrane as well (top middle panel). The merged image (top right panel) indicates that pools of the two proteins co-distribute on discrete regions of plasma membrane (arrows, indicated in yellow). As seen in Fig. 3B (lower panels), after stimulation of cells with BK, Na^+-K^+ ATPase distribution (Mobasheri et al., 1997) remains largely unchanged (bottom left panel), while plasma membrane pools of eNOS are no longer prominent (bottom middle panel). Subsequently, colocalization of the two proteins on plasma membrane is no longer detected (bottom right panel). Next, the Golgi membrane pool of eNOS was examined in an analogous manner (Fig. 3C). Under basal conditions, substantive pools of eNOS (top middle panel; arrows) reside within a perinuclear pattern reminiscent of the location of the Golgi marker, 58K protein (top left panel). Indeed, merging of these images (top right panel, yellow) demonstrates colocalization of eNOS-GFP with 58K protein. After stimulation of cells with BK, neither 58K protein (bottom left panel) or eNOS-GFP (bottom middle panel) redistribute from the Golgi membrane, as further substantiated by persistent colocalization of eNOS-GFP with Golgi 58K protein in a perinuclear distribution (bottom right panel, yellow). These observations suggest that BK stimulation of cells promotes the selective dissociation of eNOS from plasma membrane but does not promote dissociation of eNOS from Golgi.

Inhibition of GTP-dependent endocytosis, but not clathrin-dependent endocytosis, influences the subcellular redistribution of eNOS in response to BK

To test the role of dynamin and retrograde vesicle trafficking on BK-mediated internalization of eNOS, we first interrupted GTP hydrolysis within eNOS-GFP ECV 304 cells using cell permeabilization and GTP-γ-S. Cells were pre-incubated with either the cell permeant, digitonin (1 μM for 5 minutes); digitonin with the non-hydrolyzed GTP analog, GTP-γ-S; or digitonin with the non-hydrolyzed ATP analog, ATP-γ-S. Cells were stimulated with BK or vehicle and prepared for confocal imaging. The left micrograph in Fig. 4A demonstrates the plasmalemmal and perinuclear distribution of eNOS observed in cells treated with digitonin alone, which was similar to that observed in the absence of digitonin (seen in Fig. 3C, top middle panel). BK stimulation (10 μM) was associated with a decrease in the fluorescence intensity of plasmalemmal eNOS (middle micrograph), consistent with the analyses in Fig. 3. Interestingly, the influence of BK on plasmalemmal eNOS was abrogated by 5 minutes preincubation of cells with GTP-γ-s (right micrograph), though not so prominently by ATP-γ-s (not shown). Similar results were obtained in fixed BAEC, and this data was utilized for quantification of imaging as depicted in the graph in Fig. 4B. For this analysis, quantification was performed in a blind manner by assessing the percentage of cells with and without plasmalemmal eNOS after the various experimental treatments (n=200 BAEC per group in two independent experiments). Consistent with that observed qualitatively in the representative micrographs from ECV304 cells in Fig. 4A, BK stimulation of BAEC was associated with a reduction in the number of cells that expressed plasmalemmal eNOS (open bars), and this effect was abrogated by preincubation of cells with GTP-γ-s (Fig. 4B). These studies indicate that inhibition of GTP hydrolysis abrogates eNOS internalization after BK stimulation.

GTP-γ-s may inhibit both clathrin and caveolae vesicle-mediated endocytosis (Oh et al., 1998). However, as plasmalemmal eNOS resides largely within caveolae (Shaul et al., 1996), we anticipated that the inhibitory influence of GTP-γ-s on BK-mediated eNOS redistribution from the plasma

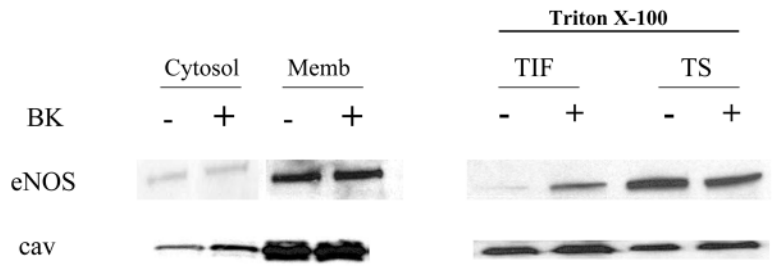

Fig. 2. BK promotes eNOS redistribution into a Triton X-100-insoluble fraction. eNOS-GFP ECV 304 cells were incubated with BK (10 μM) or vehicle for 10 minutes then fractionated into cytosol and membrane fractions. Membrane fractions were further fractionated into 0.5% Triton X-100-soluble (TS) and -insoluble fractions (TIF). eNOS protein abundance was assessed in fractions by western blot analysis. While BK stimulation did not influence the distribution of eNOS in membrane (memb) and cytosolic (cytosol) fractions (left panel), BK stimulation was associated with an enrichment of eNOS within the TIF component of the membrane fraction (right panel). Control experiments demonstrate that caveolin protein levels (cav) are enriched in membrane fractions compared to cytosol, and TIF compared to TS (lower panel). Each panel is representative of three separate experiments.

membrane was largely mediated through a caveolae-dependent process rather than via a clathrin-dependent process. To further examine this, we used complimentary pharmacological and molecular approaches, to examine a role for clathrin-dependent endocytosis in this process. First, CP, a cationic amphiphilic drug that inhibits the assembly of the clathrin adapter protein AP2 on clathrin-coated pits (Petris et al., 2002), was incubated with eNOS-GFP ECV 304 cells prior to BK stimulation. As seen in Fig. 4C, in cells preincubated with CP, internalization of eNOS-GFP is still detected in response to BK (image c; compare with cells in the absence of BK and CP in image a, and cells in the presence of BK and absence of CP in image b). Consistent with this observation, inhibition of clathrin-mediated endocytosis via the overexpression of AP 180 protein, which limits the size and distribution of clathrin cages (Ford et al., 2001), also did not prevent BK-mediated eNOS internalization (image d; compare to cells in the absence of BK in image a, and cells in presence of BK and absence of AP 180 in image b). However, AP 180 did reduce the uptake of Texas Red-conjugated transferrin from transfected cells by greater than 50% compared to cells transfected with the empty vector, indicating that this reagent was indeed functional under our experimental conditions (*n*=250 cells per group, data not shown). These studies suggest that the inhibitory influence of GTP-γ-s on BK-mediated eNOS internalization is likely a caveolae-dependent process rather than a clathrin-dependent process.

We next dissected the role of the specific cellular GTPase, dynamin-2, as this GTPase is essential to retrograde vesicle trafficking events from the plasma membrane (Dessy et al., 2000; Henley et al., 1998; Oh et al., 1998). We tested the role of dynamin in this process by overexpressing a dominant negative dynamin-2 K44A construct in eNOS-GFP ECV 304 cells, and measuring eNOS distribution within the varying buoyant density membrane fractions after BK stimulation. This construct contains a point mutation in the dynamin GTPase domain that impairs the ability of dynamin to hydrolyze GTP (Cao et al., 2000). Fig. 5A demonstrates the validity of the density gradient used in these experiments, to distinguish low and high buoyant density proteins prepared from eNOS-GFP ECV 304 cells as shown by the enrichment of the 22 kDa protein, caveolin, in the low buoyant density fractions (fractions 1-4), and the converse enrichment of the Golgi and trans-Golgi compartment marker protein, β-COP, in the high buoyant density fractions (fractions 6-7), consistent with prior studies by us and others using this technique (Peterson et al., 1999; Smart et al., 1995). After BK stimulation of eNOS-GFP ECV 304 cells transfected with empty vector, eNOS was enriched within low buoyant density fractions [Fig. 5B; *rectangular box*, see eNOS signal in lanes labeled E in fractions #1-4; (–) vs (+)], while in cells overexpressing K44A, BK-mediated enrichment of eNOS in low buoyant density fractions was not detected [Fig. 5B; rectangular box, see eNOS signal in lanes labeled K in fractions #1-4; (–) vs (+)]. Control experiments confirm overexpression of K44A as assessed by immunodetection of the V5 epitope tag (see V5 western blot band in Fig. 5B) and similar level of total proteins within each fraction as assessed by Coommassie Blue staining of gels (not shown). These studies indicate that the biochemical redistribution of eNOS in response to BK stimulation requires the GTPase function of dynamin-2.

Perturbation of GTP hydrolysis inhibits cellular NO production

We next sought to determine whether inhibition of dynamin-2-dependent vesicle trafficking might influence cellular NO production as well. First, to examine the influence of GTP-γ-s on the cellular production of NO in cells that express eNOS endogenously, BAEC were permeabilized with digitonin and pretreated with GTP-γ-s (10 μM) or vehicle. Cells were then loaded with the NO indicator dye, DAF-2DA, and BK-stimulated NO production was assessed by fluorescence microscopy. As seen in Fig. 6A (top panel micrographs), there was a time-dependent increase in cellular fluorescence intensity in response to BK. However, BK-induced NO production was markedly abrogated in cells pretreated with GTP-γ-s (middle panel micrographs in Fig. 6A), and further diminished in the presence of the NOS inhibitor, L-NAME, as well (bottom panel micrographs in Fig. 6A). Quantification of the fluorescent intensity in cells from digitized micrographs revealed a 60% decrease in NO production by GTP-γ-s in comparison to digitonin alone, in response to BK stimulation (lower graph in Fig. 6A). Next, experiments were performed to assess the effect of K44A overexpression on cellular NO production. eNOS-GFP ECV cells were transfected with empty pcDNA vector or K44A-V5 epitope-tagged vector, and cellular NO release was measured from the media using the fluorescent NO probe, DAF-2. Transfected cells were treated with either L-arginine or L-NAME and stimulated with BK or vehicle. As seen in Fig. 6B, overexpression of K44A markedly inhibited the cellular production of NO in response to BK. L-NAME inhibited NO production in all groups, indicating specificity of effect. Western blot control experiments from cell lysates, confirmed the expression of V5 epitope and overexpression of dyn-2 in cells transfected with the vector encoding K44A-V5

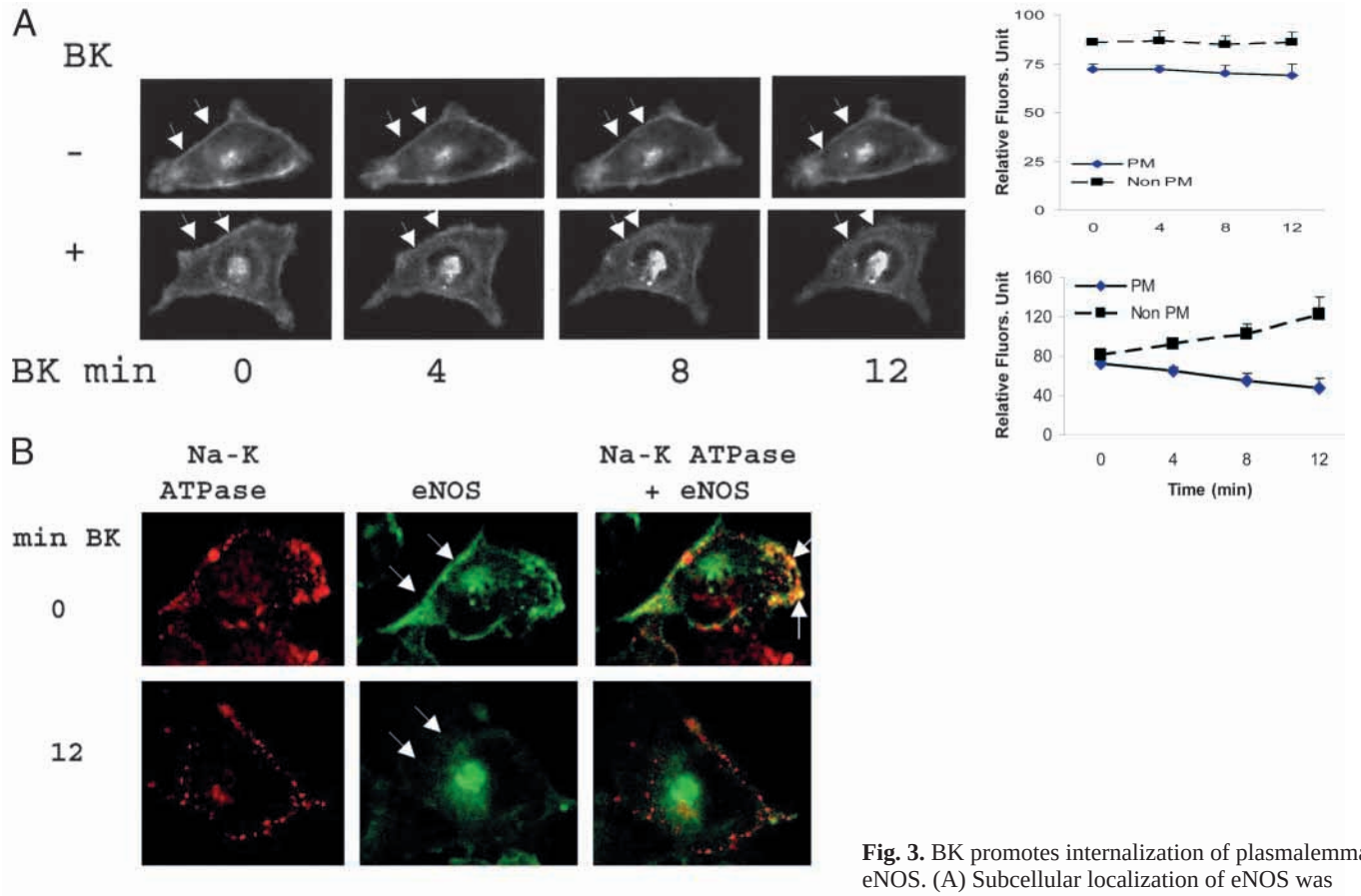

Fig. 3. BK promotes internalization of plasmalemmal eNOS. (A) Subcellular localization of eNOS was assessed by laser scanning confocal microscopy in live eNOS-GFP ECV304 cells, cultured on coverslips. Coverslips were transferred to a Zeiss temperature controlled perfusion system mounted on the microscope stage. (Top panel; BK–), eNOS-GFP was most prominent in plasma membrane and perinuclear regions of the cell, and its distribution was not influenced in the absence of BK during the 12 minutes of the experiment (arrows denote plasmalemmal eNOS). The graph accompanying the top panel quantifies the fluorescence intensity in plasma membrane (PM: solid line with diamonds) and perinuclear region (non-PM: dashed line with squares) in the sequential micrographic images. (Bottom panel; BK+), stimulation of cells with BK (10 μM) triggered a reduction in fluorescence intensity of eNOS-GFP from the plasma membrane (arrows denote distribution of plasmalemmal eNOS). The graph accompanying the bottom panel quantifies a decrease in fluorescence in PM (solid line with diamonds), but not in the perinuclear, non-PM areas (dashed line with squares). The displayed images are representative of 7 independent experiments, and the graphs were generated by compiling the data from 3 cells from each group (mean±s.e.m.). (B) Influence of BK on the distribution of Na^+-K^+ ATPase and eNOS-GFP was assessed by immunofluorescence confocal microscopy in fixed ECV304 cells. In the absence of BK stimulation, substantive pools of Na^+-K^+ ATPase (top left panel) and eNOS-GFP (top middle panel, arrows denote plasmalemmal eNOS) are detected in the cell periphery, and colocalization of discrete pools of the proteins is detected in portions of the cell periphery (top right panel, arrows denote colocalization in yellow). After BK stimulation, Na^+-K^+ ATPase remains in a plasmalemmal distribution (bottom left panel), while substantive pools of eNOS-GFP dissociate from the plasma membrane (bottom middle panel, arrows denote lack of eNOS in plasma membrane) as further evidenced by lack of colocalization with plasmalemmel Na^+-K^+ ATPase (lower right). (C) Influence of BK on the distribution of eNOS-GFP in comparison to Golgi 58K protein was assessed by immunofluorescence confocal microscopy in fixed ECV304 cells. In the absence of BK stimulation, substantive pools of 58K protein reside in a perinuclear distribution (top left panel) and pools of eNOS-GFP also reside in a perinuclear distribution (top middle panel, denoted by arrows). Colocalization of the two proteins is detected in a perinuclear Golgi pattern (top right panel, yellow). After BK stimulation of cells, 58K protein remains in a perinuclear distribution (bottom left panel), and the pool of perinuclear eNOS-GFP remains in a similar distribution (bottom middle panel), as further evidenced by maintenance of colocalization of the two proteins in a perinuclear distribution (lower right panel, colocalization denoted in yellow).

as compared to cells transfected with the empty vector, as well as similar eNOS protein levels throughout the groups. To further confirm the inhibitory influence of K44A on cellular NO production, we performed complimentary studies using NO-specific chemiluminescence, which assesses levels of the NO metabolite, nitrite. As seen in Fig. 6C, L-NAME-inhibited, BK-stimulated nitrite accumulation was reduced in cells transfected with K44A as compared to empty vector. Thus, studies using complimentary NO measurement, indicate that inhibition of cellular GTPases, particularly dynamin-2, abrogate BK-mediated NO production.

Discussion

Microscopic and biochemical analyses have previously established that eNOS protein targets to specific membrane compartments within cells and is enriched within membrane fractions of cellular lysates (Blair et al., 1999; Fulton et al., 2002; Liu et al., 1995; Prabhakar et al., 2000; Sessa et al., 1995; Shaul et al., 1996). Further membrane fractionation analyses and co-localization studies indicate that these membrane domains include plasmalemmal caveolae and Golgi membranes (Blair et al., 1999; Fulton et al., 2002; Liu et al., 1995; Prabhakar et al., 2000; Sessa et al., 1995; Shaul et al., 1996). Furthermore, the subcellular localization of eNOS appears to be a dynamic event (Michel et al., 1993). For example, photobleaching studies by Sowa et al., indicate that eNOS quickly redistributes within a specific membrane domain and that alterations in homeostatic factors, such as cell confluency, markedly influence the cellular distribution of eNOS between different compartments (Sowa et al., 1999). Other studies have demonstrated that the cellular distribution of eNOS within distinct subcellular domains is influenced by specific extracellular stimuli, some, such as BK, capable of promoting NO production (Prabhakar et al., 1998; Thuringer et al., 2002; Venema et al., 1996). For example, Prabhaker et al. and Thuringer et al., independently observed that BK promoted the distribution of cellular eNOS from

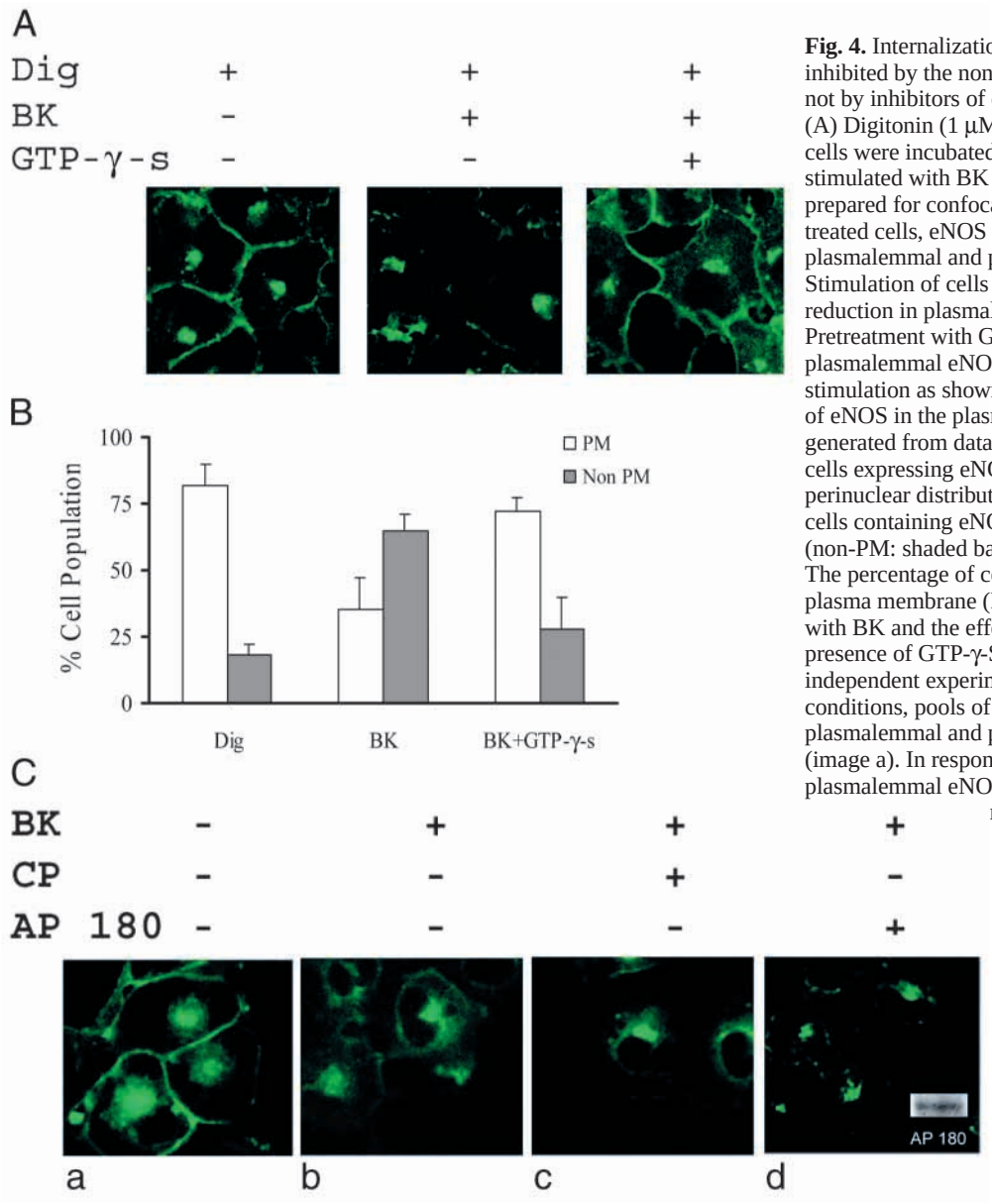

Fig. 4. Internalization of eNOS in response to BK is inhibited by the non-hydrolyzed GTP analog, GTP-γ-S, but not by inhibitors of clathrin-mediated endocytosis. (A) Digitonin (1 μM)-permeabilized eNOS-GFP ECV304 cells were incubated with vehicle or GTP-γ-S then stimulated with BK or vehicle. Cells were fixed and prepared for confocal microscopy. (Left) In digitonin-treated cells, eNOS protein was detected in a predominantly plasmalemmal and perinuclear location. (Middle) Stimulation of cells with BK (10 μM) was associated with a reduction in plasmalemmal eNOS immunostaining. (Right) Pretreatment with GTP-γ-S abrogated the internalization of plasmalemmal eNOS that was observed with BK stimulation as shown by maintenance of substantive pools of eNOS in the plasma membrane. (B) The graph, generated from data in BAEC, depicts the percentage of cells expressing eNOS in the plasma membrane and in a perinuclear distribution (PM: open bars) compared with cells containing eNOS in a perinuclear distribution only (non-PM: shaded bars), in each of the experimental groups. The percentage of cells with any amount of eNOS in plasma membrane (PM) is diminished after stimulation with BK and the effect of BK is largely abrogated in the presence of GTP-γ-S (n=200 cells in each group from 2 independent experiments; mean±s.e.m.). (C) Under basal conditions, pools of eNOS-GFP are detected in a plasmalemmal and perinuclear distribution in ECV304 cells (image a). In response to BK, internalization of plasmalemmal eNOS-GFP is detected (image b). BK-mediated eNOS-GFP internalization is not abrogated in cells pre-incubated with CP (15 μM) for 10 minutes, prior to 10 μM BK stimulation (image c). eNOS-GFP ECV304 cells were also transfected with vectors encoding myc-AP 180 or empty vector, then stimulated with BK 24 hours later. Cells for study were chosen from the myc-immunofluorescent-positive population. Despite detection of adequate levels of myc protein by western blot (image d, insert), no attenuation in BK-mediated eNOS-GFP internalization was observed (image d).

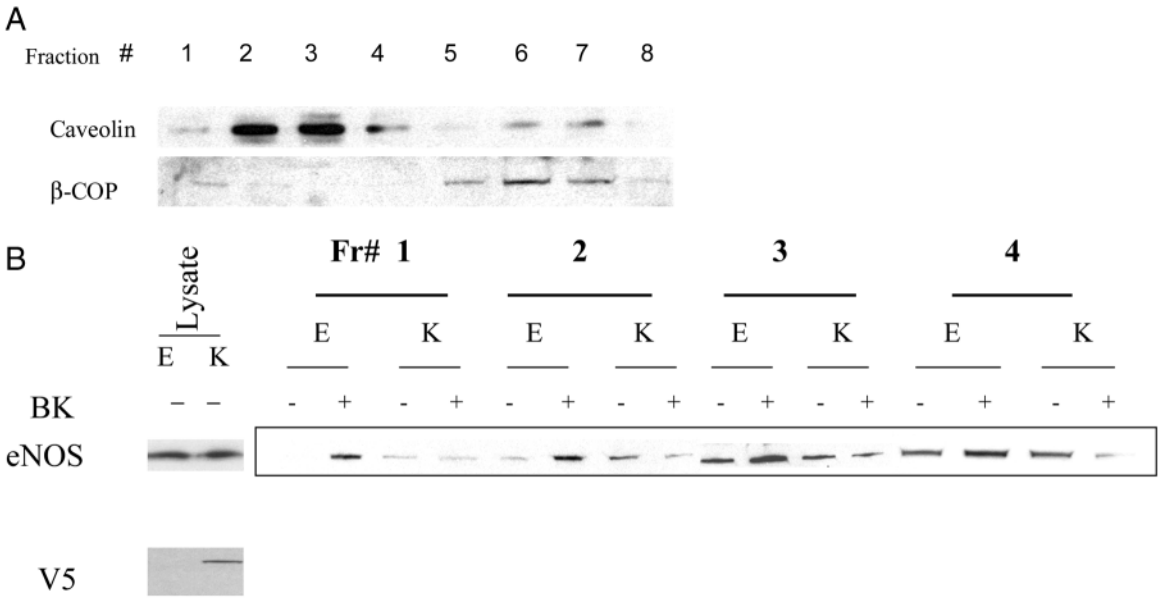

Fig. 5. Redistribution of eNOS-GFP in response to BK stimulation is abrogated by overexpression of the dominant negative dynamin-2 mutant, K44A. (A) To confirm protein separation by buoyant density gradient centrifugation, equal amounts of protein from each fraction were analyzed by SDS-PAGE and western blotting using caveolin pAb, and β-COP pAb. Enrichment of caveolin, a marker of low buoyant density cellular membranes, was detected in the early fractions (#2-4), while β-COP, a marker coat protein of Golgi and trans-Golgi, was enriched in the higher buoyant density fractions (#5-7). (B) eNOS-GFP ECV 304 cells were cotransfected with pcDNA V5 empty vector (E) or alternatively a V5 epitope-tagged dyn-2 K44A construct (K). 24 hours later, cells were stimulated with BK (10 μM for 10 minutes; +) or sham treatment (–). Four 100 mm dishes of cells from each experimental group were then prepared for sucrose gradient subcellular fractionation. Equal volumes of each fraction were analyzed for eNOS and V5-K44A expression by SDS-PAGE and western blot analysis using eNOS mAb and V5 mAb, respectively. As seen in the rectangular box in Fig. 5B, in cells transfected with empty vector (E), stimulation with BK (+), was associated with an enrichment of eNOS protein levels in the early fractions of the gradient as compared to cells in the absence of BK stimulation [see eNOS signal in lanes labeled E in fractions #1-4; (–) vs (+)]. In cells transfected with V5-K44A, the relative enrichment of eNOS in early fractions in cells after BK stimulation was no longer apparent [see eNOS signal in lanes labeled (K) in fractions #1-4; (–) vs (+)]. No major changes were observed in the distribution of eNOS in the heavy fractions in response to the various experimental conditions and Coommassie staining of SDS-PAGE gels demonstrated similar protein loading amongst the experimental groups within each fraction (not shown). Overexpression of K44A was confirmed by the detection of a 90 kDa band in total cell lysates from dishes transfected with the vector encoding V5-K44A, and overexpression did not influence total eNOS protein levels from cell lysates (see eNOS and V5 western blot bands under lanes labeled lysate). All experiments presented here were performed three times independently, with similar results.

plasmalemmal caveolae into a more diffuse intracellular localization (Prabhakar et al., 1998; Thuringer et al., 2002). Consistent with a prior study by Liu et al. (Liu et al., 1995), we did not observe a reduction in the membrane distribution of eNOS as assessed by cell fractionation analysis, but did observe a change in the biochemical characteristics of eNOS characterized by enrichment of NOS protein into Triton X-100-insoluble fractions after BK treatment, as previously noted by Venema et al. (Venema et al., 1996). In the present studies, performed with both eNOS-GFP ECV 304 cells and BAEC, which express eNOS heterologously and endogenously, respectively, BK promotes the internalization of plasmalemmal eNOS. Our studies using CP and AP 180 overexpression indicate that BK-mediated eNOS internalization is a clathrin-independent event. These studies suggest that eNOS protein accumulates within internalized caveolin-coated vesicles which have budded from the plasma membrane. However, neither the current study nor the aforementioned earlier studies on this topic have been able to fully characterize the destination of these internalized vesicles. Furthermore, stimulus-dependent eNOS internalization does not appear to be a response limited to NOS agonists as incubation of endothelial cells with OxLDL, which, conversely to BK, inhibits cellular NO production, also promotes the internalization of eNOS from its basal plasmalemmal location (Blair et al., 1999). More recent studies suggest that the NOS associated protein, NOSTRIN, may play a role in plasmalemmal eNOS internalization as well (Zimmerman et al., 2002).

The precise role of nucleotide hydrolysis and dynamin-2 in the molecular steps of membrane scission, internalization, and ensuing retrograde vesicle trafficking remain an area of active investigation (Henley et al., 1998; McNiven, 1998; Oh et al., 1998; Schnitzer et al., 1996; Schekman and Orci, 1996). In the present studies, we chose to exploit the energy requirement of vesicle trafficking to study the mechanism by which perturbation of vesicle trafficking might influence eNOS distribution and NO production by using both pharmacological and molecular approaches, in conjunction with complimentary techniques, to measure cellular NO and assess NOS localization. Indeed, a similar approach was recently utilized to dissect the role of vesicle trafficking in the desensitization of G protein-coupled receptor signaling and eNOS-caveolin

complex stability in cardiac myocytes (Dessy et al., 2000). We find that inhibition of GTP hydrolysis by GTP-γ-S impairs BK-dependent eNOS redistribution and NO production. Furthermore, perturbation of cells with dominant negative form of dynamin-2 mimic the inhibitory effects of GTP-γ-S on NO generation, indicating a particular importance of dynamin-2 in NOS trafficking and function. Dynamin-2 is of particular relevance as this protein colocalizes with caveolin and eNOS within caveolae and Golgi vesicles, and is essential in the scission and internalization of plasmalemmal vesicles (Cao et al., 2001; Henley et al., 1998; Oh et al., 1998). Our current observations are consistent with several prior studies, which have demonstrated that inhibition of dynamin GTPase function prevents internalization of caveolin-coated membrane vesicles

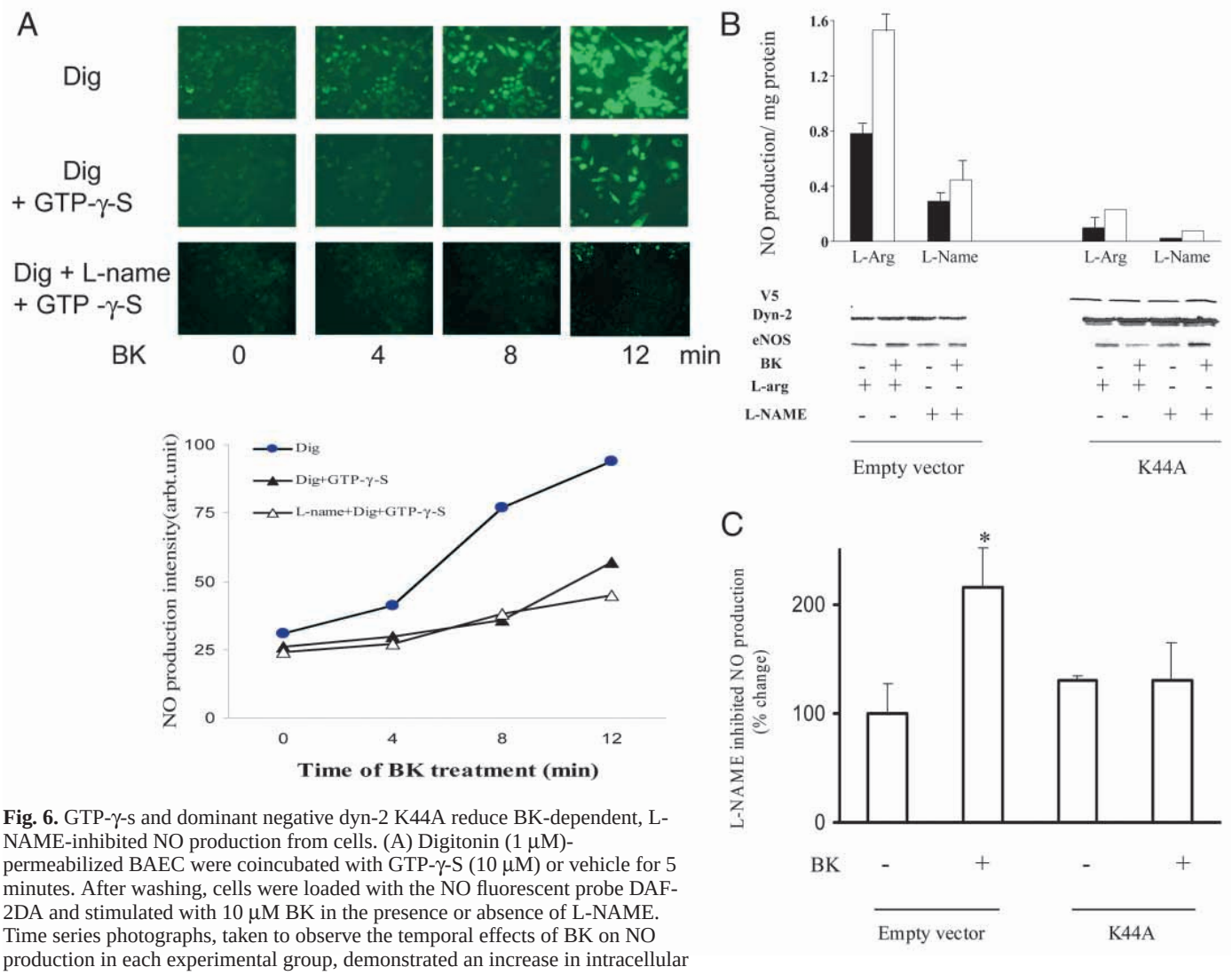

Fig. 6. GTP-γ-s and dominant negative dyn-2 K44A reduce BK-dependent, L-NAME-inhibited NO production from cells. (A) Digitonin (1 μM)-permeabilized BAEC were coincubated with GTP-γ-S (10 μM) or vehicle for 5 minutes. After washing, cells were loaded with the NO fluorescent probe DAF-2DA and stimulated with 10 μM BK in the presence or absence of L-NAME. Time series photographs, taken to observe the temporal effects of BK on NO production in each experimental group, demonstrated an increase in intracellular DAF-2DA fluorescence intensity in cells treated with BK (top panel). The increase in fluorescence intensity in response to BK was markedly abrogated in cells treated with GTP-γ-S (middle panel), or with both GTP-γ-S and L-NAME (lower panel). The graph below, depicts the quantified fluorescence intensity over time within each group and shows a significant abrogation in NO production in BK-stimulated cells incubated with GTP-γ-S or both GTP-γ-S and L-NAME as compared to BK stimulation alone. Data are representative of three independent experiments with similar results. (B) eNOS-GFP ECV 304 cells were transfected with vectors encoding V5-K44A, a dominant negative mutant of dynamin-2, or empty pcDNA3.1 vector, then serum starved for 24 hours prior to experiments. Cells were stimulated with BK or vehicle in the presence of L-arginine or L-NAME and NO release was assessed from the media using the NO probe DAF-2. After collection of media for fluorimetry, cell lysates were prepared for western blot analysis using V5 mAb, dyn-2 pAb, and eNOS mAb, as well as protein assay. In cells transfected with empty vector, BK stimulated a 2-fold increase in NO production, which was entirely inhibited in the presence of the NOS inhibitor L-NAME. Overexpression of dyn-2 K44A markedly abrogated BK stimulated NO production in the presence and absence of L-NAME. (Closed bars: 0 μM BK; open bars: 10 μM BK; n=5 independent experiments each measured in duplicate). The control immunoblot panels demonstrate overexpression of V5 epitope-tagged dyn-2 using antibodies for V5 as well as dyn-2, and similar levels of eNOS protein between the experimental groups. (C) eNOS-GFP ECV 304 cells were transfected as described above for DAF-2 fluorimetry experiments. Samples of media were collected 20 minutes after BK stimulation and analyzed for nitrite levels using NO-specific chemiluminescence. In cells transfected with empty vector, L-NAME-inhibited NO production was increased by approximately twofold in cells stimulated with BK as compared to control cells (n=3 independent experiments each analyzed with duplicate samples; *P<0.05 compared to other groups). In cells transfected with dyn-2 K44A, no prominent increase in L-NAME inhibited, BK-mediated NO production was detected.

(Henley et al., 1998; Oh et al., 1998; Pierce et al., 1999), and add to these studies by demonstrating that this process influences downstream signaling pathways, in this case relating to NOS activation. However, it is important to recognize that the influence of GTP-γ-S on eNOS trafficking may reflect inhibition of cellular GTPases in addition to dyn-2, which are essential to the processes of vesicle trafficking, such as Rab 3, Rab 5 and Rab 7 (Chavrier and Goud, 1999). Several converging and diverging BK-mediated signaling pathways that culminate in NOS activation have been well delineated (Bernier et al., 275; Harris et al., 2001; Thuringer et al., 2002; Venema et al., 1996), and the interplay of these pathways with dynamin-dependent, BK-mediated eNOS internalization will require further elucidation.

We have previously demonstrated that dynamin-2 binds in a specific manner with eNOS and promotes the catalytic activity of recombinant eNOS protein in vitro (Cao et al., 2001). In the current studies, we anticipate that K44A dynamin is likely influencing NO production through effects on vesicle internalization rather than through direct binding actions. This concept is supported by the observation that the eNOS binding domain within dynamin, resides within the carboxy-terminal proline-rich domain of dynamin-2, rather than the amino-terminal GTPase domain, wherein lies the K44A mutation (Cao et al., 2003). Furthermore, colocalization of eNOS and dynamin in cells is most prominent in the Golgi membranes (Cao et al., 2001), where a significant and bioactive pool of both proteins reside (Fulton et al., 2002), rather than within plasma membrane, where the influence of K44A appears to be most prominent. It is possible that direct binding regulation between eNOS and dynamin occurs in the Golgi membranes while dynamin-dependent endocytosis selectively influences the plasmalemmal pool of eNOS.

In conclusion, these studies, using complimentary cell lines and methodologies, demonstrate that perturbation of specific vesicle trafficking pathways has the capability to influence cellular eNOS distribution and the ensuing NO production. These studies add to the current understanding of eNOS biology by demonstrating that BK-dependent eNOS trafficking is a GTPase-dependent process, with particular importance of dynamin-2 GTPase, and that perturbation of this process impairs the cellular production of NO. Additionally, they provide further evidence that dynamin-dependent endocytosis is intimately linked to downstream cell signaling events.

These studies were supported by grants from the NIH to V.S. (R01 DK-59388, R01 DK-59615), grants from the American Heart Association to V.S. and S.C., and the Mayo Clinic Foundation. The authors acknowledge Dr M. McNiven and Dr H. McMahon for providing dynamin-2 anti-sera and the dynamin-2 K44A cDNA, and AP 180 cDNA, respectively, as well as Dr W. Sessa for providing the eNOS-GFP ECV 304 cells.

References

Bernier, S., Haldar, S. and Michel, T. (2000). Bradykinin-regulated interactions of the mitogen-activated protein kinase pathway with the endothelial nitric-oxide synthase. *J. Biol. Chem.* **275**, 30707-30715.

Blair, A., Shaul, P., Yuhanna, I., Conrad, P. and Smart, E. (1999). Oxidized low density lipoprotein displaces endothelial nitric-oxide synthase (eNOS) from plasmalemmel caveolae and impairs eNOS activation. *J. Biol. Chem.* **274**, 32512-32519.

Brown, J., Reading, S., Jones, S., Fitchett, C., Howl, J., Martin, A., Longland, C., Michelangeli, F., Dubrova, Y. and Brown, C. (2000). Critical evaluation of ECV304 as a human endothelial cell model defined by genetic analysis and functional responses: a comparison with the human bladder cancer derived epithelial cell line T24/83. *Lab. Invest.* **80**, 37-45.

Cao, H., Thompson, H., Krueger, E. and McNiven, M. (2000). Disruption of Golgi structure and function in mammalian cells expressing mutant dynamin. *J. Cell Sci.* **113**, 1993-2002.

Cao, S., Yao, J. and Shah, V. (2003) The proline-rich domain of dynamin-2 is responsible for dynamin-dependent in vitro potentiation of eNOS activity via selective effects on reductase domain function. *J. Biol. Chem.* **278**, 5894-5901.

Cao, S., Yao, Y., McCabe, T., Yao, Q., Katusic, Z., Sessa, W. and Shah, V. (2001). Direct interaction between eNOS and dynamin-2:Implications for NOS function. *J. Biol. Chem.* **276**, 14249-14256.

Chavrier, P. and Goud, B. (1999). The role of ARF and Rab GTPase in membrane transport. *Curr. Opin. Cell Biol.* **11**, 466-475.

Dessy, C., Kelly, R., Balligand, J.-L. and Feron, O. (2000). Dynamin mediates caveolar sequestration of muscarinic cholinergic receptors and alteration in NO signaling. *EMBO J.* **19**, 4272-4280.

Ford, M. G., Pearse, B. M., Higgins, M. K., Vallis, Y., Owen, D. J., Gibson, A., Hopkins, C. R., Evans, P. R. and McMahon, H. T. (2001). AP 180 recruits clathrin to membranes: structure of the ANTH domain bound to PtdIns (4,5)P_2. *Science* **9**, 1051-1055.

Fulton, D., Fontana, J., Sowa, G., Gratton, J.-P., Lin, M., Li, K.-X., Michell, B., Kemp, B., Rodman, D. and Sessa, W. (2002). Localization of endothelial nitric-oxide synthase phosphorylated on serine 1179 ane nitric oxide on Golgi and plasma membrane defines the existence of two pools of active enzymes. *J. Biol. Chem.* **277**, 4277-4284.

Goetz, R., Thatte, H., Prabhakar, P., Cho, M., Michel, T. and Golan, D. (1999). Estradiol induces the calcium-dependent translocation of endothelial nitric oxide synthase. *Proc. Natl. Acad. Sci. USA* **96**, 2788-2793.

Harris, M., Ju, H., Venema, V., Liang, H., Zou, R., Michell, B., Chen, Z., Kemp, B. and Venema, R. (2001). Reciprocal phosphorylation and regulation of endothelial nitric-oxide synthase in response to bradykinin stimulation. *J. Biol. Chem.* **276**, 16587-16591.

Henley, J., Krueger, E., Oswald, B. and McNiven, M. (1998). Dynamin-mediated internalization of caveolae. *J. Cell Biol.* **141**, 85-99.

Kojima, H., Nakatsubo, N., Kikuchi, K., Sawahara, S., Kirino, Y., Nagoshi, H., Hirata, Y. and Nagano, T. (1998). Detection and imaging of nitric oxide with novel fluorescent indicators: diaminofluoresceins. *Annal. Chem.* **70**, 2446-2453.

Liu, J., Garcia-Cardena, G. and Sessa, W. (1995). Biosynthesis and palmitoylation of endothelial nitric oxide synthase: mutagenesis of palmitoylation sites, cysteine-15 and/or –26, argues against depalmitoylation-induced translocation of the enzyme. *Biochemistry* **34**, 12333-12340.

McNiven, M. (1998). Dynamin: a molecular motor with pinchase action. *Cell* **94**, 151-154.

Michel, T., Li, G. K. and Busconi, L. (1993). Phosphorylation and subcellular translocation of endothelial nitric oxide synthase. *Proc Natl. Acad. Sci. USA* **90**, 6252-6256.

Mobasheri, A., Errington, R. J., Golding, S., Hall, A. C. and Urban, P. G. (1997). Characterization of the Na+,K+-ATPase in isolated bovine articular chondrocytes; molecular evidence for multiple and isoforms. *Cell Biol. Int.* **21**, 201-212.

Oh, P., McIntosh, P. and Schnitzer, J. E. (1998). Dynamin at the neck of caveolae mediates their budding to form transport vesicles by GTP-driven fission from the plasma membrane of endothelium. *J. Cell Biol.* **141**, 101-114.

Palmer, R., Ferrige, A. and Moncada, S. (1987). Nitric oxide release accounts for the biological activity of endothelium-derived relaxing factor. *Nature* **327**, 524-526.

Papapetropoulos, A., Rudic, R. and Sessa, W. (1999). Molecular control of nitric oxide synthases in the cardiovascular system. *Cardiovasc. Res.* **43**, 509-520.

Paxinou, E., Weisse, M., Chen, Q., Souza, J., Hertkorn, C., Selak, M., Daikhin, E., Yudkoff, M., Sowa, G., Sessa, W. et al. (2001). Dynamic regulation of metabolism and respiration by endogenously produced nitric oxide protects against oxidative stress. *Proc. Natl. Acad. Sci. USA* **98**, 11575-11580.

Peterson, T., Poppa, V., Ueba, H., Wu, A., Yan, C. and Berk, B. (1999). Opposing effects of reactive oxygen species and cholesterol on endothelial nitric oxide synthase and endothelial cell caveolae. *Circ. Res.* **85**, 29-37.

Petris, M. J., Smith, K., Lee, J. and Thiele, D. J. (2002). *J. Biol Chem.* **278**, 9639-9646.

Pierce, K., Maudsley, S., Daaka, Y., Luttrell, L. and Lefkowitz, R. (1999). Role of endocytosis in the activation of the ERK cascade by sequestering and nonsequestering G protein-coupled receptors. *Proc. Natl. Acad. Sci. USA* **97**, 1489-1494.

Prabhakar, P., Cheng, V. and Michel, T. (2000). A chimeric transmembrane domain directs endothelial nitric-oxide synthase palmitoylation and targeting to plasmalemmel caveolae. *J. Biol. Chem.* **275**, 19416-19421.

Prabhakar, P., Thatte, H., Goetz, R., Cho, M., Golan, D. and Michel, T. (1998). Receptor-regulated translocation of endothelial nitric-oxide synthase. *J. Biol. Chem.* **273**, 27383-27388.

Rudic, R. (1998). Direct evidence for the importance of endothelium-derived nitric oxide in vascular remodeling. *J. Clin. Invest.* **101**, 731-736.

Schekman, R. and Orci, L. (1996). Coat proteins and vesicle budding. *Science* **271**, 1526-1533.

Schnitzer, J., Oh, P. and McIntosh, D. (1996). Role of GTP hydrolysis in fission of caveolae directly from plasma membranes. *Science* **274**, 239-242.

Sessa, W. C., Garcia-Cardena, G., Liu, J., Keh, A., Pollock, J. S., Bradley, J., Thiru, S., Braverman, I. M. and Desai, K. M. (1995). The Golgi association of endothelial nitric oxide synthase is necessary for the efficient synthesis of nitric oxide. *J. Biol. Chem.* **270**, 17641-17644.

Shah, V., Haddad, F., Garcia-Cardena, G., Frangos, J., Mennone, A., Groszmann, R. and Sessa, W. (1997). Liver sinusoidal endothelial cells are responsible for nitric oxide modulation of hepatic resistance. *J. Clin. Invest.* **100**, 2923-2930.

Shah, V., Toruner, M., Haddad, F., Cadelina, G., Papapetropoulos, A., Sessa, W. and Groszmann, R. (1999). Impaired endothelial nitric oxide synthase activity associated with enhanced caveolin binding in experimental liver cirrhosis. *Gastroenterology* **117**, 1222-1228.

Shaul, P. (2002). Regulation of endothelial nitric oxide synthase: location, location, location. *Annu. Rev. Physiol.* **64**, 749-774.

Shaul, P., Smart, E., Robinson, L., German, Z., Yuhanna, I., Ying, Y., Anderson, R. and Michel, T. (1996). Acylation targets endothelial nitric-oxide synthase to plasmalemmal caveolae. *J. Biol. Chem.* **271**, 6518-6522.

Smart, E., Ying, Y., Mineo, C. and Anderson, R. (1995). A detergent-free method for purifying caveolae membrane from tissue cultured cells. *Proc. Natl. Acad. Sci. USA* **92**, 10104-10108.

Sowa, G., Liu, J., Papapetropoulos, A., Rex-Haffner, M., Hughes, T. and Sessa, W. (1999). Trafficking of endothelial nitric-oxide synthase in living cells. *J. Biol. Chem.* **274**, 22524-22531.

Thuringer, D., Maulon, L. and Frelin, C. (2002). Rapid transaction of the vascular endothelial growth factor receptor KDR/Flk-1 by the bradykinin B2 receptor contributes to endothelial nitric-oxide synthase activation in cardiac capillary endothelial cells. *J. Biol. Chem.* **277**, 2028-2032.

Venema, V., Marrero, M. and Venema, R. (1996). Bradykinin-stimulated protein tyrosine phosphorylation promotes endothelial nitric oxide synthase translocation to the cytoskeleton. *Biochem. Biophys. Res. Commun.* **226**, 703-710.

Zimmerman, K., Opitz, N., Dedio, J., Renne, C., Muller-Esterl, W. and Oess, S. (2002). NOSTRIN: A protein modulating nitric oxide production and subcellular distribution of eNOS *Proc. Natl. Acad. Sci. USA* **99**, 17167-17172.